J Comput Aided Mol Des (2011) 25:825–835
DOI 10.1007/s10822-011-9466-5

Substrate binding to mammalian 15-lipoxygenase

Lea Toledo · Laura Masgrau · José M. Lluch · Àngels González-Lafont

Received: 16 March 2011 / Accepted: 8 August 2011 / Published online: 23 August 2011

Abstract Lipoxygenases (LOs) are implicated in the regulation of metabolic processes and in several human diseases. Revealing their exact role is hindered by an incomplete understanding of their activity, including substrate specificity and substrate alignment in the active site. Recently, it has been proposed that the change in substrate specificity for arachidonic acid (AA) or linoleic acid (LA) could be part of an auto-regulatory mechanism related to cancer grow. Kinetic differences between reactions of 15-hLO with AA and LA have also led to the suggestion that the two substrates could present mechanistic differences. In the absence of a crystal structure for the substrate:15-LO complex, here we present an atomic-level study of catalytically competent binding modes for LA to rabbit 15-LO (15-rLO-1) and compare the results to our previous work on AA. Docking calculations, molecular dynamics simulations, re-docking and cross-docking calculations are all used to analyze the differences and similarities between the binding modes of the two substrates. Interestingly, LA seems to adapt more easily to the enzyme structure and differs from AA on some dynamical aspects that could introduce kinetic differences, as observed experimentally. Still, our study concludes that, despite the different chain lengths and number of insaturations between these two physiological substrates of 15-rLO-1, the enzyme seems to catalyze their hydroperoxidation by binding them with a common binding mode that leads to similar catalytically competent complexes.

Keywords Lipoxygenases · Linoleic acid · Molecular dynamics · Docking · Binding mode · Specificity

Electronic supplementary material The online version of this article (doi:10.1007/s10822-011-9466-5) contains supplementary material, which is available to authorized users.

L. Toledo · J. M. Lluch · À. González-Lafont
Departament de Química, Universitat Autònoma de Barcelona, 08193 Bellaterra, Barcelona, Spain

L. Toledo · L. Masgrau (✉) · J. M. Lluch · À. González-Lafont (✉)
Institut de Biotecnologia i de Biomedicina (IBB), Universitat Autònoma de Barcelona, 08193 Bellaterra, Barcelona, Spain
e-mail: laura.masgrau@uab.cat

À. González-Lafont
e-mail: angels@klingon.uab.es

Introduction

Lipoxygenases (LOs) are nonheme iron-containing enzymes that catalyze the hydroperoxidation of polyunsaturated fatty acids including a 1,4-cis,cis-pentadiene motif. They are vital enzymes for the regulation of metabolic processes and, in mammals, LOs products are implicated in several diseases such as asthma, psoriasis, atherosclerosis and cancer [1]. Therefore, they are of interest as targets in drug design. Revealing the exact role of LOs in human disease is hampered by an incomplete understanding of LOs activity, including substrate specificity, substrate alignment in the active site and allosteric regulation [2, 3]. Recently, the substrate specificity (arachidonic acid, AA vs. linoleic acid, LA) of the human 15-hLO isozymes has been suggested to be relevant in cancer progression [4]. Significant differences between reaction of 15-hLO with AA or LA have also been reported by the measured kinetic isotope effects (KIEs) on k_{cat} and k_{cat}/K_M [3, 4]. The generally accepted catalytic reaction for this enzyme (Scheme 1) involves a hydrogen transfer that is thought to be the rate-determining (RDS) step. The latest

studies on 15-hLO-1, though, have shown that multiple RDS can be implicated at low temperatures (a hydrogen-bond rearrangement and a hydrogen abstraction). The contribution of each step seems to change with the substrate: for LA, the H-transfer clearly dominates the mechanism and presents a much higher KIE (indicative of hydrogen tunneling) than for AA. The work of Holman and coworkers concluded that there are mechanistic differences with the two substrates (LA and AA), even though hydrogen atom tunneling may be a common feature [4].

From the structural point of view, the crystal structure of rabbit reticulocyte 15-rLO-1 with and without an inhibitor bound (PDB entry code 2P0M) [5] is available, showing an important conformational change of the enzyme upon ligand binding. This conformational transition mainly affects the α2-, α3- and α18-helixes. In addition, mutagenesis studies have revealed the importance of Phe353, Ile418, Met419, Ile593 and Arg403 (15-rLO-1 numbering) in regiospecificity [6, 7]. The first residues are thought to define the depth of the active site, where the methyl end of the substrate would be situated, whereas Arg403, at the entrance of the active site, would interact with the carboxylate end. In two previous studies an homology model of 15-hLO-1 was built using the revised 15-rLO-1 structure as a template [8, 9]. In the first work, AA and LA were successfully docked by Holman et al. [8] in the closed 15-hLO-1 and the modes of binding obtained for both substrates were said to be consistent with mutagenesis experiments. More recently, Mascayano et al. [9] carried out a steered molecular dynamics study of the unbinding process of AA and two inhibitor molecules from 12-hLO to 15-hLO-1. From the docking of the substrate into the active site of the modeled 15-hLO-1, some relevant interactions are highlighted: an electrostatic interaction between AA carboxylic group and the amino group of Arg402 at one end, and a hydrophobic interaction between Phe414 and the other AA chain end. Beyond this data, however, there is no direct molecular structural evidence on catalytically productive LO-fatty acid complexes so that the substrate alignment at the (relatively big) active site remains rather speculative [10]. Moreover, as new LOs crystal structures are published, [11] it seems that this feature could not be shared between different LO families. The knowledge of how different substrates accommodate in the active sites of LOs is vital for the understanding of positional specificity in these enzymes. We have recently presented [12] a theoretical study of AA binding to 15-rLO-1; our results support the sometimes referred as boot-shaped cavity for the 15-rLO-1:AA complex as a plausible AA binding mode ready for catalysis. The next question, then, is whether the chemical and structural differences between the two physiological substrates of 15-rLO-1, LA and AA, lead to different binding modes and catalytically competent complexes or not.

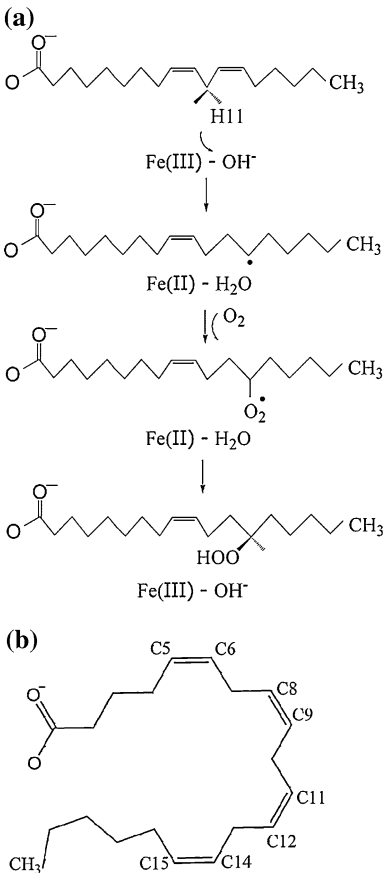

Scheme 1 **a** Mechanism of linoleic acid hydroperoxidation by 15-lipoxygenase and **b** arachidonic acid representation

Here, we present an atomic-level study of the binding modes of LA to rabbit reticulocyte 15-rLO-1 and compare the results with our recent work on 15-rLO-1:AA, searching for similarities and differences between the two substrates at this stage of the mechanism. We focus our attention on complexes consistent with known mutagenesis data and ready for hydrogen abstraction (pre-catalytic or catalytically competent complexes). We combine protein–ligand dockings, molecular dynamics simulations and re-docking calculations on representative protein structures selected from the simulations (the latter is used to both, introduce the effect of protein flexibility and to evaluate the suitability of the inhibitor-bound crystal structure in binding the substrate). We have also performed cross-docking studies with AA and LA in order to investigate further the binding modes of the two substrates and the induced-fit effect provoked by their binding. Finally, we have carried out an *in silico* experiment to investigate the possible involvement of a network of H-bonds in the α2-helix conformational change.

Computational methods

The general protocol used here resembles that of our recent work on 15-rLO-1:AA complexes [12]. However, we have gone one step further in order to compare the binding modes of the two 15-rLO-1 physiological substrates (LA and AA): we have performed a clustering analysis of the substrate alignment in the active site obtained in the simulations of the two substrates, and we have also carried out a cross-docking analysis. The details of the calculations are given in this section.

Docking, molecular dynamics simulations and re-docking

In order to generate 15-rLO-1:LA complexes, protein–ligand dockings were first carried out with the Autodock-v4.0 program [13]. The coordinates of the inhibitor-bound monomer of 15-rLO-1 (PDB entry code 2P0M) were used for the receptor. For the setup of the receptor, an oxidation state of III was assigned to the iron, as it is in the active form of the enzyme and the hydroxide anion was modeled (Scheme 1). The protonation state of the ionizable residues was determined with the PROPKA program as well as by visual inspection. The protein and ligand structures were prepared with AutoDock Tools. For the standard atoms, the Kollman united-atom partial charges were used. As these charges are not defined for the iron and its coordination environment, partial charges derived from our previous [12] M05/LANL2DZ quantum mechanics electronic structure calculations on a model cluster of the Fe^{3+} and its coordination sphere were assigned to these atoms. The calculated NPA charges (1.365 au for Fe, −0.910 au for O, and 0.524 au for H) were assigned to the iron and the hydroxide ion. The remaining excess charge needed to fulfill the classical charge of +1 for the iron, and its first coordination sphere was distributed among the rest of the coordinating atoms. For the ligand, the Kollman united-atom partial charges were used. A total of 14 torsional bonds were allowed to rotate during the docking process. The grid maps were calculated using AutoGrid4.0, with 126 × 106 × 126 points and a grid point spacing of 0.153 Å. These values were chosen so that the whole active site, which is quite big, was considered in the calculations. The docking calculations were run with the Lamarckian Genetic Algorithm in Autodock4.0, which combines a genetic algorithm and an adaptative local search algorithm. A total of 100 runs were launched. Most of the parameters for the genetic algorithm were set to the default values recommended by the program, except for the maximum number of energy evaluations and generations, which were set to larger values (2.5×10^6 and 2.7×10^5, respectively) to account for the degrees of freedom of the system under study and were at the limit of the combinatorial explosion. Analysis of these results led to the selection of an enzyme:substrate pre-catalytic structure. The positioning of LA with respect to the above mentioned residues as well as the distance of the C11 carbon atom to the OH^- group (from the Fe(III)–OH^- cofactor), were considered in the analysis. This 15-rLO-1:LA complex was used as the starting point for two 4 ns-molecular dynamics simulations (LA-1 and LA-2) carried out in order to relax the whole solvated system. The two simulations differ in the assignment of initial velocities. The CHARMM-version c35 program was used, [14] with the CHARMM-22 force field parameters [15, 16] for the protein atoms, and with the parameters specifically developed by Saam et al. [17] for the 15-rLO-1:AA system for the iron and its first coordination sphere. The force field topology and parameters for the LA ligand were derived from the lipids CHARMM-27 ones [18]. The crystallographic water molecules were added to the enzyme:substrate complex and the missing hydrogens were built with the HBUILD facility in CHARMM. The system was then solvated with a 117 Å × 82 Å × 70 Å box of preequilibrated TIP3P waters. The total charge of the system was neutralized with the addition of seven sodium cations. The resulting solvated enzyme:substrate complex had a total of ∼72,100 atoms, with ∼10,600 of them belonging to the 663 residues of the protein. The system was submitted to some energy minimization steps. MD simulations under periodic boundary conditions (PBCs) were then started. The system was gradually heated from 20 to 298 K in a time period of 365 ps, followed by a trajectory of 300 ps to ensure equilibration. During the heating and the first part of the equilibration, the C11–OH^- distance [*d*(C11–OH)] was restrained to the corresponding value obtained in the docking solution. Those restraints were gradually released, and a production period of 4 ns was run. All of the simulations were done at constant pressure and temperature (CPT), using the extended system constant pressure and the Hoover constant temperature algorithms. A time step of 2 fs was used. All of the angles and bonds involving hydrogen atoms were constrained by the SHAKE algorithm. The PBCs were built with the CRYSTAL module of CHARMM using an orthorhombic unit cell. The Particle Mesh Ewald method for long-range electrostatics was used. A total of six representative protein structures were then selected from the molecular dynamics simulations and were used to redock LA into 15-rLO-1. This is an approach used in docking calculations in order to account in some way for the protein flexibility. Further details on the docking and molecular dynamics procedures can be found in Ref. [12].

The capability of the unbound 15-rLO-1 crystal structure (monomer A in 2P0M) for accepting the substrates has

also been assessed by performing docking calculations of both LA and AA to this enzyme conformation.

Substrate clustering and cross-docking

In order to better compare the binding modes of LA and AA we have performed a clustering of the substrate coordinates obtained in the present and previous molecular dynamics simulations. The results facilitate a better visualization of the alignment adopted by each substrate in the 15-rLO-1 active site. All the analysis of the simulations have been carried out with the CHARMM modules, except the clustering analysis, for which we have used the g_cluster tool in GROMACS [19] with the so-called Gromos method [20]. We have also introduced a re-docking step in which the representative protein coordinates obtained from the molecular dynamics simulations of one substrate were used to dock the other substrate, and vice versa. The results of this cross-docking, together with the re-docking and the docking ones, provide us with information about how differently 15-rLO-1 adapts to the two substrates when they are bound in the active site.

In silico mutagenesis experiment

Several residues forming a H-bond network that could be involved in the α2-helix conformational change were identified here and in our previous work [12]. Mutants of these residues were generated *in silico* with the program Chimera, [21] by changing the residue side-chain and searching for the best rotamer in each case. The wild type monomer B in 2P0M and the mutant enzymes were then submitted to 4-ns molecular dynamics simulations following the procedure described before. In this case, though, no substrate was present in the active site. The conformation adopted by the α2-helix along these simulations was analyzed.

Results and discussion

LA binding to the 15-rLO-1 crystal structure

Docking of LA to the bound crystal structure results in a considerable number of different binding modes, with a couple of them presenting the carboxylate end buried inside the cavity (in the vicinity of the metal center or at the bottom of the cavity). It is worth noticing that, although an orientation with the carboxylate in the vicinity of the metal ligands is not consistent with mutagenesis data for LA or AA binding and reactivity, such orientation resembles the binding mode of the RS7 inhibitor found in the crystal structure (Fig. 1a). Virtual screening studies on 15-hLO have also found similar interactions for some of the potential inhibitors tested [22]. Therefore, the possibility of such interactions, although not relevant for AA or LA reaction, may be an aspect to consider in the design of new 15-LO ligands.

The docking results also show binding modes that are in qualitative agreement with the experimental mutagenesis data (Fig. 1b). Among them, we find the best model in terms of predicted binding affinity (-7.07 kcal mol^{-1}).

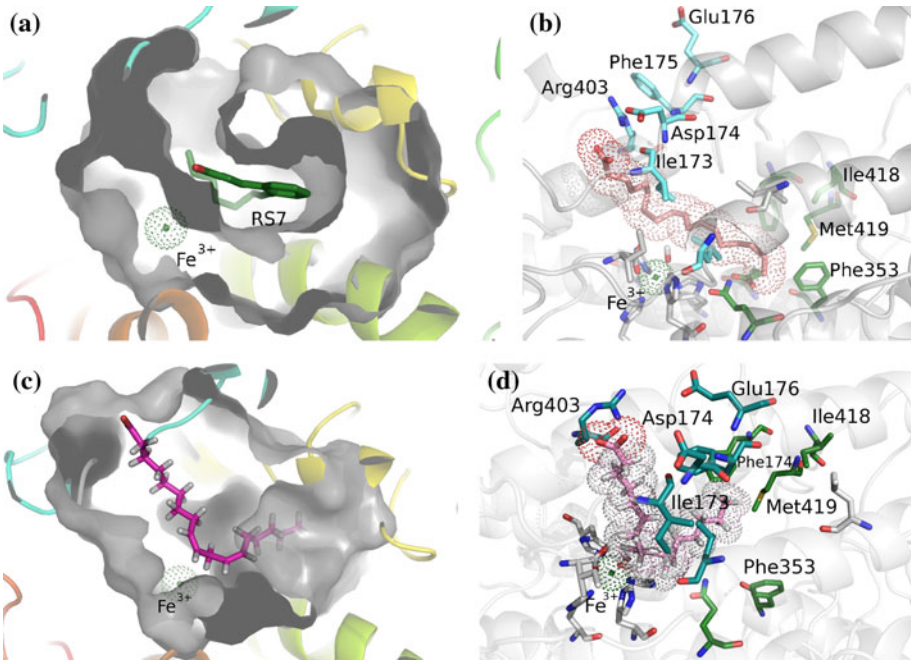

Fig. 1 Representation of the active site cavity for **a** the crystal structure (2P0M, chain B), **b** the docking solution used as a starting point of the molecular dynamics simulation of the 15-rLO-1:LA complex, and **c**, **d** a representative snapshot from the LA-1 simulation. These pictures were produced with the program Pymol

Table 1 Summary of the docking calculations to the crystal structures, the re-docking calculations to enzyme snapshots from the simulations and the cross-docking calculations (italicized), for LA and AA as ligands

	Unbound crystal structure	Inhibitor-bound crystal structure	*LA-1*	*LA-2*	*M-F4*	*M-F4-S*	*M-F4-S2*
LA	3/6	10/59	36/43	11/12	*12/13*	*37/40*	*12/20*
AA	0/3	3/38[a]	*30/42*	*18/26*	10/15[a]	24/28[a]	9/17[a]

For each calculation, a X/Y ratio is given, where Y indicates the number of models out of 100 with the reactive *d(C–OH)* distance <4.5 Å, and X corresponds to the number of those models which also have the substrate carboxylate at less than 4.0 Å of Arg403

[a] From Ref. [12]

This value is slightly higher than the one predicted for AA (-7.24 kcal mol^{-1}) [12]. Remarkably, 59 out of the 100 models generated have *d(C11–OH)* < 4.5 Å, which could be considered a plausible docking solution for abstraction of the corresponding H11 by the OH^- group. However, only 10 models out of the 59 have also the carboxylate end close to the Arg403 (at less than 4.0 Å, Table 1). A similar trend was obtained in our previous work for the docking of AA to 15-rLO-1, although LA seems to fit better in the crystal structure active site than AA. In fact, for AA the ratio of positive hits was very low (38 models with C13, the carbon atom equivalent to C11 in LA, close to the OH^- group but only 3 with also the AA carboxylate interacting with Arg403). The shorter chain length and the lower number of insaturations in LA with respect to AA could be the cause of these differences by making LA more adaptable and facilitating its positioning in the active site cavity. In fact, in a work by Kühn et al. [23] it was proven that 11,14-C20:2 binds to 15-rLO-1 and shows an activity comparable to LA. Hence, the difference between LA and AA was not attributed to the length itself of those two substrates but to the rigid character of the four almost planar pentadienes in AA making less favorable its packing in the binding pocket.

The docking calculations to the unbound form of 15-rLO-1 (monomer A in 2P0M) are much less successful in terms of catalytically competent complexes found, both for LA and AA (Table 1 and Fig. S1). This indicates that the inhibitor-bound conformation is better for accommodating the substrate.

15-rLO-1 adapts to the presence of LA

Although the inhibitor-bound form seems to be a more reliable structural model for hosting the substrate in its active site our molecular dynamics simulations introduce important changes, so indicating that the inhibitor-bound structure is still not the optimal for correctly binding the substrate. Inspection of the inhibitor-bound crystal structure reveals that the Arg403 sidechain interacts with the Asp174 carboxylate and the backbone carbonyl of Ile173 (Fig. 1b). These H-bonds partially block the entrance to the active site cavity and are, in part, responsible for the low number of docking models obtained with the LA carboxylate interacting with Arg403. According to the simulations of the 15-rLO-1:LA complex presented here, these interactions disappear when the 15-rLO-1:LA complex is allowed to relax (Fig. 1d). During the LA-1 molecular dynamics simulations, these two interactions are lost and Arg403 substitutes them for a H-bond with Glu176 and one with the ligand carboxylate, interactions not found in the inhibitor-bound crystal structure. For binding of AA, the same structural changes were obtained. In addition, in the LA-2 simulation the α2-helix opens up as it did in the M-F4-S simulation of the 15-rLO-1:AA complex (see Fig. 4 in Ref. [12]). This conformational change was proposed to be correlated with the lack of the Arg403–Glu176 hydrogen bond by the interference of the fatty acid (see below) [12]. In simulation LA-2, the Arg403 rotates and encounters another hydrogen bond partner in Glu399, while keeping the interaction with the LA carboxylate.

As can be seen in Table 1, when LA is docked to relaxed protein structures obtained from the LA-1 simulation, the number of catalytically competent complexes (C11 close to the OH^-) and interacting with Arg403 is much higher than when docked to the crystal structure. Among other factors, the new environment of Arg403 favors its interaction with the substrate carboxylate which, in turn, facilitates the right alignment of LA in the active site. Similar conclusions were drawn from the AA re-docking calculations [12]. When the enzyme structures are taken from the LA-2 simulation, though, there is no clear improvement over the crystal structure results (see Table 1). We have analyzed these results and found that, in this case, the new environment of Arg403 also increases the number of docking solutions presenting the Arg403 interaction with the LA carboxylate. However, most of these solutions have the C11 atom too far from the OH^- group, probably as a result of the rotation of Arg403 mentioned above.

In our previous work on AA, we showed that the consideration of several protein structures obtained in the simulations for the (re)docking calculations resulted in an enrichment of positive solutions (catalytically competent

complexes). This confirmed that the simulations generate enzyme structures more adapted to the substrate present in its active site and that the crystal structure was not optimal. The re-docking results presented here for LA point out in the same direction. Therefore, our results indicate that the Arg403 region in the crystal coordinates is not structurally ready for binding neither LA nor AA. And maybe even more importantly, they show that 15-rLO-1 is able to adapt to the nature/shape of the ligand, which is a dynamical aspect that should be taken into account in drug design projects targeting this family of enzymes.

Comparison of the LA and AA binding modes

If 15-rLO-1 presents conformational differences depending on the ligand bound in its active site, then the question arises on whether LA and AA, both physiological substrates of the enzyme, share or not their binding mode and the conformational changes induced to the enzyme. To compare the structures of the catalytically competent complexes obtained for AA and LA we have carried out a clustering of the LA structures sampled along the molecular dynamics simulations. We have done the same analysis for the AA simulations of our previous work. The protein alpha carbons were used for initial alignment of all the structures and a Root Mean Square Fluctuation (RMSF) cutoff of 1.7 Å was used for clustering the ligands. This procedure resulted in a few number of highly populated clusters (and several low populated ones), which show us the main orientations adopted by LA and AA in the 15-rLO-1 active site of these complexes (Fig. 2a). In the case of AA one populated cluster was identified for each trajectory whereas for LA two populated clusters were found for LA-1 and only one populated cluster for LA-2 trajectory. As can be seen, LA and AA share a common overall orientation in the relatively big 15-rLO-1 active site cavity. This orientation is in agreement with the experimental mutagenesis data. The main differences in the clustering appear at the tail of the fatty acids. This is especially the case for the pink and light green clusters, which give an idea of the space actually available for the substrates. The carboxylate region is more conserved, although some differences can be seen as a result of the position of Arg403 and the particular interaction made with it in each case. Therefore, Fig. 2a shows that there is a common main orientation for both 15-rLO-1 physiological substrates. In order to assess which contacts both AA and LA make with the protein, a contact analysis for LA has also been carried out along the two generated trajectories in this work, and a comparison with the corresponding AA analysis [12] has been made. The results of those contact analysis are shown in Fig. 2b–g for both substrates, and in Table 2 for LA and Table S1 of Ref. [12] for AA. As it was

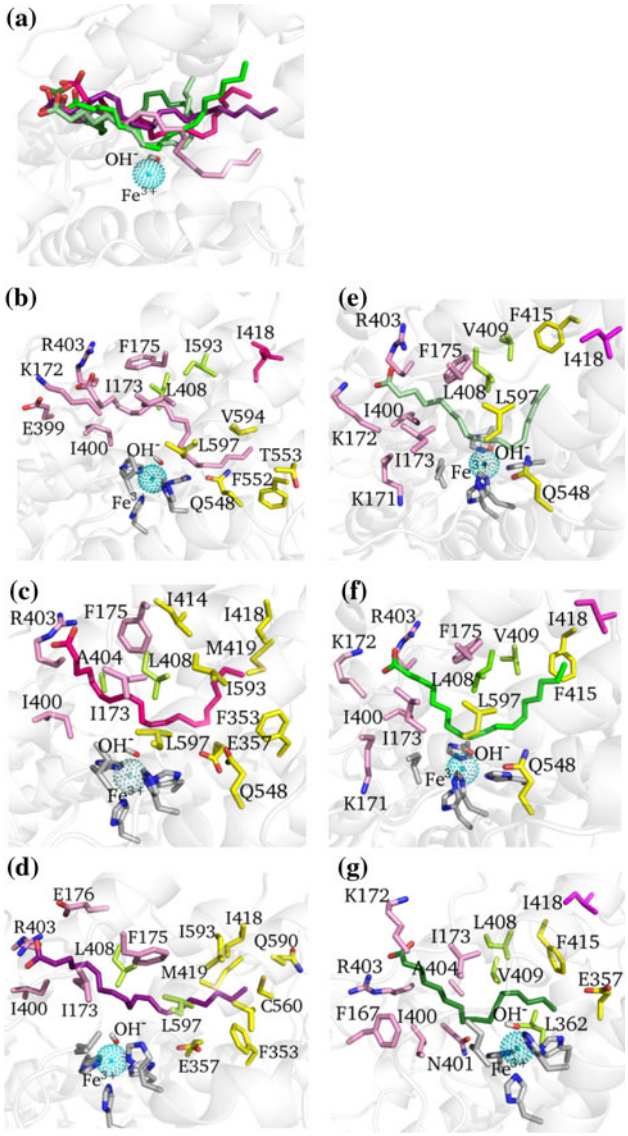

Fig. 2 **a** Main orientations adopted by AA (*purple, magenta and pink*) and LA (*light, grass and dark green*) in the 15-rLO-1 active site along the molecular dynamics simulations and obtained by clustering; **b, c, d** Representation of the active site residues that surround AA according to the contact analysis results corresponding to trajectories named as M-F4, M-F4-S and M-F4-S2, respectively; **e, f, g** Representation of the active site residues that surround LA according to the contact analysis results corresponding to trajectories named LA-1 (**e, f**) and LA-2 (**g**). The iron is depicted as a *sphere* surrounded by its ligands. Residues in different zones are depicted in different colors for facilitating visualization. *Pink* I418 is used to locate the bottom of the cavity. Hydrogen atoms are not shown for clarity. These pictures were produced with the program Pymol

already highlighted in our previous study, AA is well-wrapped by quite a large number of protein residues inside the cavity. For M-F4 (Fig. 2b) the contacts at the chain end are established with Gln548, Phe552, Thr553, Val594, and Leu597, whereas for M-F4-S and M-F4-S2 structures it is shown in Fig. 2c–d that the bottom of the cavity is defined

by Phe353, Glu357, Ile414, Ile418, Met419, Gln590, Ile593, Val594, and Leu597. In the middle part Leu408, Leu597 (in M-F4-S and M-F4-S2) and Ile593 (in M-F4) as well as the iron center and its coordination residues are the contacts of the protein with the substrate for the AA structures. At the entrance of the cavity the contacts are mainly established between AA and Arg403, Ile400, Ileu173, Lys172, and Phe175. For LA, the contact analysis obtained along the LA-1 trajectory is shown in the first column of Table 2, and depicted for the corresponding clusters in Fig. 2e and f. The bottom of the cavity for LA is defined by Phe415, Gln548 and Leu597. In the middle part Leu408 and Val409 are the contacts of the protein with LA and at the entrance of the cavity the contacts are mainly established with Arg403, Ile400, Lys171, Lys172 and Ileu173. Along the LA-2 trajectory the contact analysis (second column of Table 2, Fig. 2g) reveals that the bottom of the cavity is defined by Glu357, Leu362 and Phe415. In the middle part we find Leu408 and Val409, and at the entrance of the cavity there are contacts of LA with Arg403, Ile400, Asp401, Ala404, Phe167, Lys172 and Lys173. The comparison between the contact analysis results of AA and LA reveals less contacts for the shorter substrate. However, when re-docking calculations are carried out using the enzyme structures obtained along these molecular dynamics simulations, the same main binding mode is recovered (see Fig. S1), giving consistency to this model of catalytically competent complex for both substrates.

Table 2 Contact analysis of LA along the 4-ns trajectories

	LA-1	*LA-2*
Phe167	–	C2,C3,C4
Lys171	C2	
Lys172	C1,O1,O2	C2,C3
Ile173	C1,O1,C2,C3	C1,O1,C2,C3,C4
Phe175	C2,C3,C4,C6	–
Glu357	–	C17,C18
His361	–	C18
Leu362	–	C14,C15,C16,C17,C18
His366	–	C8,C9,C10,C11
Ile400	C3,C4,C5	C5,C6,C7,C8,C9,C10
Asp401	–	C9,C10,C11
Arg403	C1,O1,O2,C2,C3	C1,O1,O2,C2,C3,C4,C5
Ala404	–	C9,C10,C11,C12,C13,C14
Leu408	C11,C14	C13,C14,C15
Val409	C17, C18	C14,C15
Ile414	–	–
Phe415	C18	C15,C16,C17
Ile418	–	–
His545	C9,C10	–
Gln548	C11,C12,C13	–
Leu589	–	–
Gln590	–	–
Ile593	–	–
Leu597	C11,C12	–
Ile663	C7,C8,C9,C10	C7,C8,C9,C10,C11,C12
OH^-	C9,C10,C11,C12	C12

A distance cutoff of 5.0 Å was used (non-hydrogen atoms). The LA atoms involved in the contact are listed. Only occupancies higher than 0.6 are considered

As indicated above, in this work the re-docking experiments were taken one step further by exchanging the ligand and receptor structures (cross-docking). The results are also summarized in Table 1 (italicized) and some structures are shown in Fig. S1. As can be seen, for a given set of enzyme structures (one column) the number of positive hits is similar with the two substrates, although LA tends to give slightly better results. This indicates that the structural changes induced by LA binding are equivalent to those provoked by AA binding. Therefore, and even though LA and AA have a different number of carbon atoms and of insaturations, 15-rLO-1 catalyzes their hydroperoxidation by binding them in the same orientation.

Some dynamical considerations

Among the different parameters analyzed from the simulations, the reactive distance *d(H11–OH)* is an important one for evaluating the suitability of the model as a catalytically competent complex. It is worth reminding that we are using a force-field description of the system and that we have not imposed any restrain on this distance along the 4 ns production runs. The reactive distances *d(H11–OH)* along simulations LA-1 and LA-2 have been monitored and are presented in Fig. 3. This parameter shows interesting differences between LA and AA. For LA-2 both *d(H11–OH)* distances remain relatively short during the production run, with average values of *d(H11A–OH)* = 4.1 ± 0.6 Å and *d(H11B–OH)* = 3.3 ± 0.5 Å. For LA-1, the production run starts at longer distances, which become shorter as the enzyme: LA complex relaxes with the progression of the simulation. Their average values are 5.1 ± 0.9 and 4.8 ± 1.0 Å for H11A and H11B, respectively, over the full 4 ns simulation. If we only take the data for the last 2 ns, the average values are then even shorter (4.7 ± 0.9 and 4.2 ± 1.0 Å for H11A and H11B, respectively). Comparison with the equivalent distances for AA (*d(H13–OH)*), reveals that for LA the reactive hydrogen tends to be closer to the OH^- group. The 15-rLO-1:AA simulation with the shortest average *d(H13–OH)* distance (simulation M-F4-S2 in Ref. [12]) has values of 5.5 ± 0.9 and 6.1 ± 0.8 Å for H13A and H13B, respectively. The next closest values correspond to simulation M-F4, and are 6.0 ± 1.3 and 6.4 ± 1.5 Å for *d(H13A–OH)* and

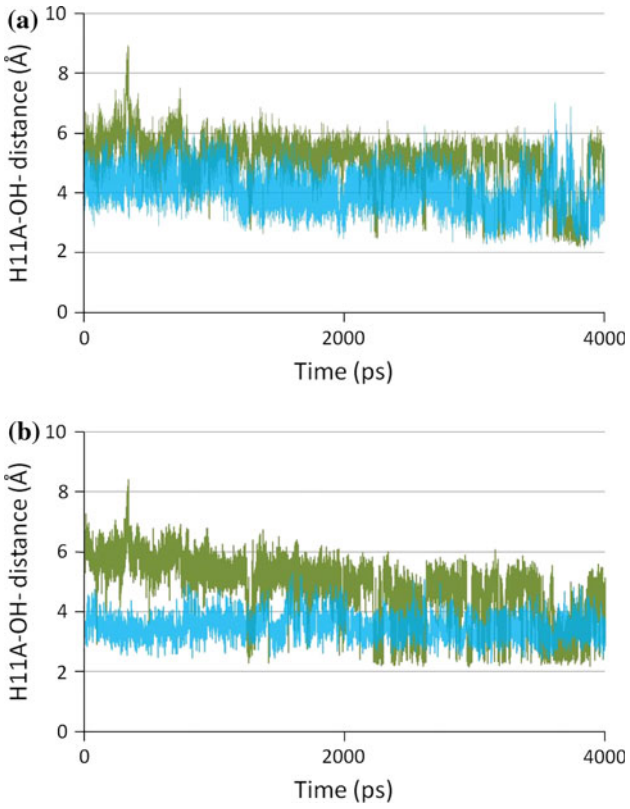

Fig. 3 Time series of the distance between (a) H11A or (b) H11B and the OH^- group along the 4-ns simulations: LA-1 (green) and LA-2 (blue). Distances are in Å and time in ps

d(H13B–OH), respectively. Finally, the largest values in the 15-rLO-1:AA simulations are of 6.5 ± 1.1 and 6.4 ± 1.2 Å for *d(H13A–OH)* and *d(H13B–OH)*, respectively (simulation M-F4-S in Ref. [12]).

The comparison of the 15-rLO-1:LA and 15-rLO-1:AA simulations also reveals an interesting difference in the dynamical behavior of the two substrates (Fig. 4). The RMSF values for LA are relatively small (1.0–1.5 Å), constant along most of the fatty acid chain but they increase at the tail (especially for LA-2, in agreement with the clustering analysis). For AA, the RMSF values tend to be higher (1.5–2.5 Å, except for the M-F4 carboxylate head which has lower values) and, more interestingly, they change abruptly at several points of the chain. Again, this seems to be a consequence of the lower number of insaturations in LA. In fact, we already noticed in our work on AA that the rigidity introduced by the double bonds could make that a rotation around one of the fatty acid single bonds resulted in a significant spatial rearrangements at other points of the chain (see Fig. S6 in the Electronic Supplementary Material of Ref. [12]). Differences in the dynamics of the two substrates may give rise to differences in the macroscopic kinetic parameters, especially if hydrogen tunneling has a major role in the reaction.

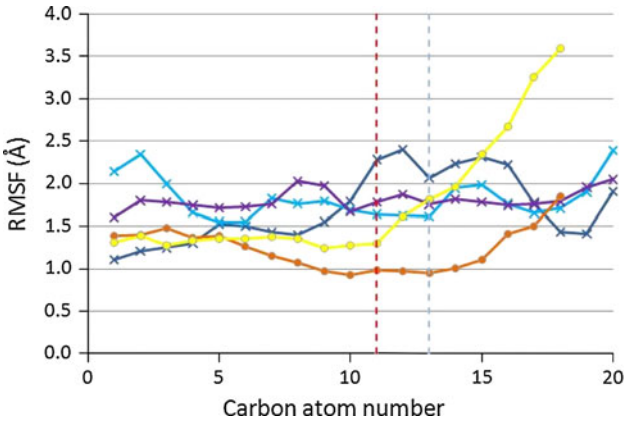

Fig. 4 Root mean squared fluctuations (RMSF, in Å) of the substrate carbon atoms during the 15-rLO-1:LA simulations LA-1 (*orange*) and LA-2 (*yellow*) from this work, and the 15-rLO-1:AA simulations M-F4 (*dark blue*), M-F4-S (*light blue*) and M-F4-S2 (*purple*) from Ref. [12]. The C11 and C13 locations are signaled with *vertical broken lines*

Therefore, our simulations show that the two 15-rLO-1 physiological substrates (AA and LA) can lead to different proton donor–acceptor distances when forming complexes with 15-rLO-1, in such a way that a significant change in the corresponding KIEs could be expected, as observed experimentally. However, the final effect of the difference observed in the dynamical fluctuations and *d(H–OH)* distances on the reaction rate and the KIEs are not easy to predict a priori [24–26]. This is especially true when the hydrogen transfer is dominated by vibration-driven tunneling mechanism, as it is suspected to be the case here and as it has been proven for soybean lipoxygenase-1 [27].

Conformational change of the α2-helix

One of the main structural differences between the inhibitor bound and the unbound crystal structures for 15-rLO-1, corresponds to the location of the α2-helix. In most of the simulations we have carried out on the 15-rLO-1:substrate complexes, the overall position of this helix stays the same as in the inhibitor bound crystal structure, although some changes in H-bonds are observed at the base of the helix. In two of the simulations, though, the α2-helix exhibits a significant conformational change that resembles the movement needed to reach the unbound form of the enzyme. In our recent work on AA [12] we proposed that the lost of H-bonds between some residues at the base of the helix (Asp174 and/or Glu176) and the helix lying in front of it, which contains Arg403, could be part of the mechanism for the conformational change observed upon ligand binding. This proposal was motivated by the observation of this structural correlation in our simulations. The same apparent correlation has been observed in the

present work. In order to further investigate this hypothesis, we have carried out an *in silico* mutagenesis experiment with the inhibitor-bound crystal structure in which the mentioned H-bonds have been eliminated from the enzyme. In particular, we have built the R403L mutant, and the D174A/E176A double mutant and have run molecular dynamics simulations of them. We removed the substrate from the active site to avoid the carboxylate interference. The expected results were that the α2-helix would open-up as there are no H-bonds holding the two enzyme parts together. However, the analysis of the simulations has shown that it stayed closed (Fig. 5). Therefore, it seems that the breaking of this H-bond network alone is not able to provoke the conformational change observed for the α2-helix, at least in the absence of the substrate, so then, other factors might be contributing. We have to remark that a MD simulation starting from the inhibitor-bound crystal structure, having removed the inhibitor and without introducing any substrate (therefore, an apo-enzyme), does not produce the change of the α2-helix either. In this case, however, with respect to the x-ray structure, Arg403 loses its hydrogen bond with Asp174 although it maintains the one with Ile173.

In our previous work [12] some flexibility was also observed for the α18-helix in addition to some degree of correlation between those α18 movements and those of the substrate, so that our conclusion was that the enzyme adapts to the position of the ligand. The correlation between the α2 and the α18 movements upon ligand binding would need of further analysis out of the scope of the present paper.

Transferability of the results to the 15-hLO-1

In order to assess how transferable our results on 15-rLO-1 are to the human counterpart, a homology model of 15-hLO-1 has been built using the 2P0M monomer B coordinates as a template. Alignment between human and rabbit 15-LO-1 sequences has been performed using the ClustalW approach [28] in the Jalview environment [29] (see Electronic Supplementary Material Fig. S2). Conservation between both enzymes is very high, with a sequence identity of 81%. The homology model has been generated using the Modeller program [30] and both, alignment and structures, have been analyzed using the UCSF Chimera environment. A selection of residues within 7 Å of the docked substrates has been compared; only six of these residues are different between the two species (see Fig. 6). Two of them differ in one carbon atom (rI173/hV172 and rT553/hS552) and are found at the carboxylate-bound region and at the bottom of the binding site, respectively. Another two present an extra hydroxyl group for the human enzyme (rF552/hY551 and rV594/hT593); these two residues, together with hS552, lie at the bottom end of the active site cleft and only the AA tail is observed to contact them in some of our simulations (see Supporting Information Table S4 in Ref. [12] and Table 2 here). hY551 could be able to establish an hydrogen bonds with a carboxylate-first bound substrate; however, the salt bridge with hR402 is expected to be stronger and, in fact, docking calculations made by other groups on a homology model of 15-hLO-1 predict a tail-first binding mode for AA, ruling out this possibility. The two lasting differences (rK172/hR171 and rN406/hT405) are found at the surface of the protein and are solvent exposed. They both conserve charge, polar character and H-bond ability (although with some differences). Summarizing, the high sequence identity between 15-hLO-1 and 15-rLO-1, together with the low and quite conservative mutations observed between the two species in the binding site cavity, suggest that the

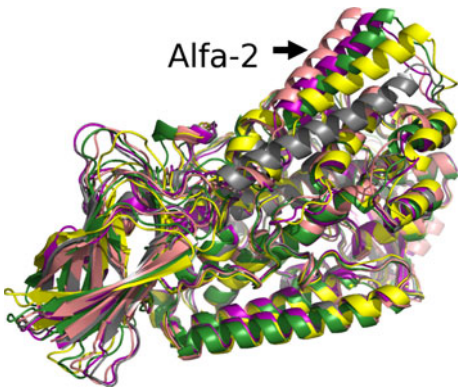

Fig. 5 *Ribbon* representation of 15-rLO-1 showing the conformation adopted by the α2-helix in the inhibitor-bound crystal structure (*purple*), the unbound crystal structure (*gray*), simulation LA-2 (*yellow*) and simulation of the R403L (*pink*) and the D174A//E176A (*green*) mutants

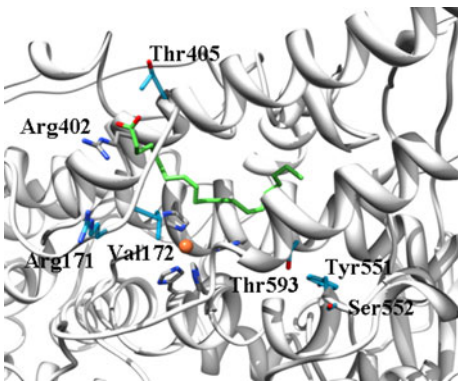

Fig. 6 Representation of the 15-hLO-1 homology model showing in *blue sticks* the active site residues that differ in sequence from the 15-rLO-1 and that are found within 7 Å of the docked substrate. The iron cation is shown as a *sphere*, and the residues coordinating it and hArg402 (rArg403) in *grey sticks*. One of the arachidonic acid docked solutions (in r-15LO-1) is depicted in *green sticks*. Hydrogens are not shown for clarity

conclusions drawn in this work about AA and LA binding to 15-rLO-1 are also valid for the human enzyme.

Conclusions

Our results show that the inhibitor-unbound monomer of the heterodimer contained in the crystal structure (PDB entry 2P0M) of the 15-rLO-1 is not suited to accommodate none of its physiological substrates, LA and AA. On the contrary, the inhibitor-bound monomer of the crystal structure, that includes a significant conformational change of the α2-helix, seems to be a more reliable structural model for hosting the substrate in the active site. The Arg403 region (near the surface of the enzyme) in that crystal structure is not ready for binding neither LA nor AA yet. However 15-rLO-1 is flexible enough to adapt to the substrate by means of a reorganization of the hydrogen-bond network in that region and sometimes by the displacement of the α2-helix. Very interestingly, AA and LA share a similar overall binding mode to 15-rLO-1 although some local differences exist. As a matter of fact, the hydrogen atoms that are abstracted in the initial step of the hydroperoxidation mechanism are attached to both C13 and C10, two of the bisallylic methylene carbon atoms of AA while the hydrogens that are captured when LA is the substrate are bonded to C11, the unique bisallylic methylene carbon atom. The carboxylate head of the fatty acids interact with Arg403, whereas the methyl ends lie in the nearby of Ile418 and Met419, as has been inferred from experimental mutagenesis data. The overall position for the carboxylate head is more conserved between different simulations but the methyl end shows some more flexibility, especially for LA, which also presents smaller fluctuations at the reaction center. For AA, the fluctuations of the carbon atoms are more irregular along the chain. These differences are attributed to a more rigid central part in AA with its four insaturations and a shorter chain for LA by two carbon atoms. The analysis of the catalytically competent complexes obtained for 15-rLO-1 with these two substrates also reveals an interesting trend: the LA substrate is better positioned for reaction (shorter *d(H–OH)* distances) in such a way that a significant change in the corresponding KIEs can also be predicted. However, the final effect of the differences observed in the dynamical fluctuations and *d(H–OH)* distances on the reaction rate and the KIEs are not easy to predict a priori. This is especially true when the hydrogen transfer is dominated by vibration-driven tunneling mechanism, as it is suspected to be the case here and as it has been proven for soybean lipoxygenase-1.

The work here presented provides a structural model for further interpretation and generation of experimental data that leads to a better understanding of the LOs implication and regulation of disease. From the computational point of view, the next step will be to carry out a complete quantum mechanical study of the corresponding chemical reactions taking into account all the structural and dynamical aspects discussed in this work. Such a study is now in progress in our laboratory.

Acknowledgment We thank the financial support from the Spanish "Ministerio de Ciencia e Innovación" through project CTQ2008-02403/BQU and the "Ramon y Cajal" program (L.M.), and "Generalitat de Catalunya" project 2009SGR409. We are especially grateful to Professor H. Kühn and Dr. J. Saam for kindly providing us with the force field parameters for the iron and its first coordination sphere ligands. The authors are very grateful to J.-D. Maréchal for his help with the homology model of 15-hLO-1.

References

1. Kühn H, Saam J (2005) Free Radic Biol Med 39:S4
2. Ivanov I, Heydeck D, Hofheinz K, Roffeis J, O'Donnell VB, Kühn H, Walther M (2010) Arch Biochem Biophys 503:161–174
3. Jacquot C, Wecksler AT, McGinley CM, Segraves EN, Holman TR, van der Donk WA (2008) Biochemistry 47:7295–7303
4. Wecksler AT, Jacquot C, van der Donk WA, Holman TR (2009) Biochemistry 48:6259–6267
5. Choi J, Chon JK, Kim S, Shin W (2008) Proteins: Struct Funct Bioinformatics 70:1023–1032
6. Borngraber S, Browner M, Gillmor S, Gerth C, Anton M, Fletterick R, Kühn H (1999) J Biol Chem 274:37345–37350
7. Schwarz K, Borngraber S, Anton M, Kühn H (1998) Biochemistry 37:15327–15335
8. Wecksler AT, Kenyon V, Deschamps JD, Holman TR (2008) Biochemistry 47:7364–7375
9. Mascayano C, Núñez G, Acevedo W, Rezende M (2010) J Mol Model 16:1039–1045
10. Vogel R, Jansen C, Roffeis J, Reddanna P, Forsell P, Claesson H-E, Kühn H, Walther M (2010) J Biol Chem 285:5369–5376
11. Gilbert NC, Bartlett SG, Waight MT, Neau DB, Boeglin WE, Brash AR, Newcomer ME (2011) Science 331:217–219
12. Toledo L, Masgrau L, Maréchal JD, Lluch JM, González-Lafont À (2010) J Phys Chem B 114:7037–7046
13. Morris GM, Huey R, Lindstrom W, Sanner MF, Belew RK, Goodsell DS, Olson AJ (2009) J Comput Chem 30:2785–2791
14. Brooks BR, Brooks CL, Mackerell AD, Nilsson L, Petrella RJ, Roux B, Won Y, Archontis G, Bartels C, Boresch S, Caflisch A, Caves L, Cui Q, Dinner AR, Feig M, Fischer S, Gao J, Hodoscek M, Im W, Kuczera K, Lazaridis T, Ma J, Ovchinnikov V, Paci E, Pastor RW, Post CB, Pu JZ, Schaefer M, Tidor B, Venable RM, Woodcock HL, Wu X, Yang W, York DM, Karplus M (2009) J Comput Chem 30:1545–1614
15. MacKerell AD, Bashford D, Bellott M, Dunbrack RL, Evanseck JD, Field MJ, Fischer S, Gao J, Guo H, Ha S, Joseph-McCarthy D, Kuchnir L, Kuczera K, Lau FTK, Mattos C, Michnick S, Ngo T, Nguyen DT, Prodhom B, Reiher WE, Roux B, Schlenkrich M, Smith JC, Stote R, Straub J, Watanabe M, Wiorkiewicz-Kuczera J, Yin D, Karplus M (1998) J Phys Chem B 102:3586–3616
16. MacKerell AD, Feig M, Brooks CL (2004) J Comput Chem 25:1400–1415
17. Saam J, Ivanov I, Walther M, Holzhutter HG, Kühn H (2007) Proc Natl Acad Sci USA 104:13319–13324

18. Feller SE, MacKerell AD (2000) J Phys Chem B 104:7510–7515
19. Hess B, Kutzner C, van der Spoel D, Lindahl E (2008) J Chem Theory Comput 4:435–447
20. Daura X, Gademann K, Jaun B, Seebach D, van Gunsteren WF, Mark AE (1999) Angew Chem Int Ed 38:236–240
21. Pettersen EF, Goddard TD, Huang CC, Couch GS, Greenblatt DM, Meng EC, Ferrin TE (2004) J Comput Chem 25:1605–1612
22. Kenyon V, Chorny I, Carvajal WJ, Holman TR, Jacobson MP (2006) J Med Chem 49:1356–1363
23. Kühn H, Sprecher H, Brash AR (1990) J Biol Chem 265:16300–16305
24. Tejero I, Garcia-Viloca M, González-Lafont À, Lluch JM, York DM (2006) J Phys Chem B 110:24708–24719
25. Mavri J, Liu HB, Olsson MHM, Warshel A (2008) J Phys Chem B 112:5950–5954
26. Ranaghan KE, Masgrau L, Scrutton NS, Sutcliffe MJ, Mulholland AJ (2007) ChemPhysChem 8:1816–1835
27. Edwards SJ, Soudackov AV, Hammes-Schiffer S (2010) J Phys Chem B 114:6653–6660
28. Thompson JD, Higgins DG, Gibson TJ (1994) Nucleic Acids Res 22:4673–4680
29. Waterhouse AM, Procter JB, Martin DMA, Clamp M, Barton GJ (2009) Bioinformatics 25:1189–1191
30. Sali A, Blundell TL (1993) J. Mol Biol 234:779–815